

Production of Alfvén Waves by a Rapidly Expanding Dense Plasma

M. VanZeeland,¹ W. Gekelman,¹ S. Vincena,¹ and G. Dimonte²

¹Department of Physics and Astronomy, University of California, Los Angeles, California 90095

²Lawrence Livermore National Laboratory, Livermore, California 94550

(Received 23 March 2001; published 17 August 2001)

The expansion of a dense (initially, $n_{\text{lpp}}/n_0 \gg 1$) laser-produced plasma into an ambient magnetized plasma ($n_0 = 2 \times 10^{12} \text{ cm}^{-3}$) capable of supporting Alfvén waves has been studied. The interaction results in the production of shear Alfvén waves as well as large density perturbations ($\Delta n/n_0 \sim 0.3$) associated with the moving dense plasma. The waves propagate away from the target and are observed to become plasma-column resonances. Spatial patterns of the wave magnetic fields are measured and are used to estimate the coupling efficiency of the laser energy and the kinetic energy of the dense plasma into wave energy.

DOI: 10.1103/PhysRevLett.87.105001

PACS numbers: 52.35.Bj, 94.20.Bb, 96.60.Wh

The basic physics of a high-beta, spatially localized plasma expanding into an ambient plasma and the consequent radiation of wave energy is fundamental in many areas of space and plasma physics. In solar physics, coronal mass ejections may play a key role in the dynamics of space weather and the origin of turbulence in the solar wind [1,2]. In laboratory fusion experiments, some tokamaks are fueled by pellet injection—a method which can often cause disruptions [3,4]. Also in tokamaks, transport studies have been done using laser-ablation plasmas in which the expanding plasma was observed to cause hydro-magnetic activity [5–7]. In the Earth’s ionosphere, the 1962 detonation of a 1.5 Megaton nuclear device at an altitude of 400 km (project STARFISH) may have disabled a power station as a result of intense wave propagation to the ground [8–10]. In this Letter, we report the generation and observation of radiation from a rapidly expanding ($v_{\text{expan}}/v_{\text{Alfvén}} \sim 0.1\text{--}1$), high density (initially, $n_{\text{lpp}}/n_0 \gg 1$) laser-produced plasma (lpp) embedded in an ambient, steady state, fully magnetized plasma (He, $n = 2 \times 10^{12} \text{ cm}^{-3}$, 10 m long, 40 cm diam, $B_0 = 1.2 \text{ kG}$). The experiment is performed in the Large Plasma Device (LAPD) at UCLA [11]. A schematic of the experiment is shown in Fig. 1. Previous Alfvén wave experiments in this machine involved wave generation by antennas and skin depth scale currents [12–14]. In this experiment, the wave generation mechanism is significantly different.

The laser-produced plasma is generated by the irradiation of a 1.9 cm diameter cylindrical aluminum target with a 1.5 J, 7 ns, temporal Gaussian profile, Nd-YAG laser focused to a spot (size $< 1 \text{ mm}$). The laser is fired at the same, 1 Hz, repetition rate as the plasma. To present a fresh surface to the laser, the target, located 5.66 m from the cathode, is rotated and/or translated along its axis every five shots using a dual stepper motor system. The lpp’s expansion into a vacuum was diagnosed previously using an angular array of Faraday cups with $B_0 = 0$ [15]. The plasma was found to contain 2.5×10^{15} particles with velocity $v_{\parallel} = 1.4 \times 10^7 \text{ cm/s}$ parallel to the laser beam (normal to the target surface) and $v_{\perp} = 1.1 \times 10^7 \text{ cm/s}$

in the perpendicular direction. This represents a total lpp kinetic energy of $E_{\text{lpp}} \sim 0.7 \text{ J}$, or one-half of the laser energy. The expansion velocities are consistent with those obtained from gated optical images and scaling laws [16]. With $B_0 = 1.2 \text{ kG}$, the lpp expands as follows: the Al ions are unmagnetized with a directed Larmor radius of $\sim 24 \text{ cm}$ whereas the electrons are magnetized with a Larmor radius of $< 1 \text{ mm}$. Without a background plasma, the electrons are pulled across the magnetic field to neutralize the ions by a strong electric field. This produces a self-consistent $\vec{E} \times \vec{B}$ current which completely expels the magnetic field. This lpp diamagnetic cavity expands until the total excluded magnetic energy becomes comparable to E_{lpp} , namely, to a magnetic confinement radius $R_b = (12E_{\text{lpp}}/B_0^2)^{1/3}$, where $E_{\text{lpp}} = 0.75 \times 10^7 \text{ ergs}$ and the factor of 12 is due to expansion from a flat surface into 2π steradians. The average deceleration is $g \sim v_{\perp}^2/2R_b$ and the time to stagnation is $\sim 2R_b/v_{\perp}$. The diamagnetic cavity then recoils to the initial state and the lpp begins to expand along the magnetic field. The result is a large amplitude, spatially localized impulse to the background magnetic field ($\delta B/B = 1$) and background plasma ($\delta n/n = 1$). With a background plasma present, the cross-field neutralization of the energetic Al ions is more complex because background electrons can flow down the magnetic

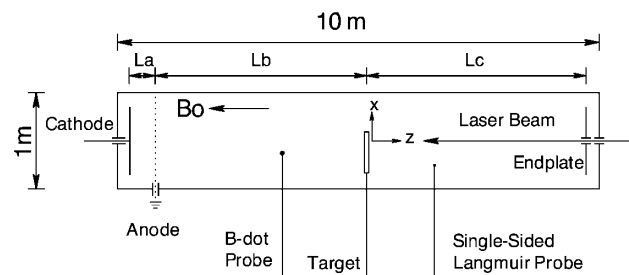


FIG. 1. Schematic of the experimental setup. The single-sided Langmuir probe and B -dot probe can be placed at different positions both radially and axially. The coordinate system used is centered where the laser strikes the target. $L_a = 62 \text{ cm}$, $L_b = 566 \text{ cm}$, $L_c = 329 \text{ cm}$.

field lines. This will reduce the self-consistent $\vec{E} \times \vec{B}$ current in the lpp which will reduce the plasma diamagnetism. In addition, the parallel current in the background plasma will generate Alfvén waves. This has been verified in a recent computer simulation in which waves with $B_{\perp} \approx 2$ G were observed for our experimental conditions [17].

Figure 2 shows the temporal profile of the current density collected using a single-sided Langmuir probe (area = 1 mm^2) facing the expansion plasma taken at $x = 0 \text{ cm}$, $y = -0.75 \text{ cm}$, $z = 62 \text{ cm}$ (the origin is defined to be the laser impact position). The initial high frequency spikes are due to fast particles and secondary emission caused by x rays [18]. The lpp begins to arrive $5 \mu\text{s}$ after the laser is fired and the peak density arrives approximately $7.5 \mu\text{s}$ later, giving a speed of $5.0 \times 10^6 \text{ cm/s}$. This is less than 50% of the initial expansion velocity. Also, the lpp has a peaked profile with a radius of approximately 1 cm , which is $R_p/4$. This is due to the collapse of the diamagnetic cavity and the forward-directed nature of the lpp from a flat surface.

The interaction between the expanding dense plasma and the background produces waves over a large frequency spectrum. They are observed both above and below the helium ion cyclotron frequency. In this paper we investigate Alfvén waves in the vicinity of the ion cyclotron frequency of the background plasma. The magnetic fields of the waves are obtained with an inductive pickup probe consisting of three orthogonal coils. The density pertur-

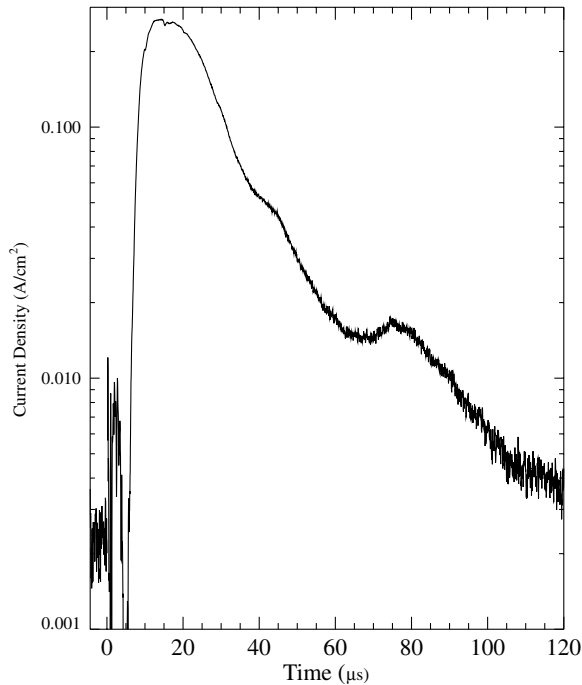


FIG. 2. The temporal evolution of the current density as measured with the single-sided Langmuir probe drawing ion saturation current $x = 0$, $y = -0.75 \text{ cm}$, $z = 62 \text{ cm}$. The signal at $t < 0$ is due to the background He plasma. The flux arriving at $t > 5 \mu\text{s}$ is due to the dense, fast moving Al plasma.

bations associated with the waves are measured using a single-sided Langmuir probe collecting ion saturation current. Data are acquired in several planes perpendicular to the background magnetic field on a $30 \text{ cm} \times 24 \text{ cm}$ xy grid with $\Delta x = \Delta y = 0.75 \text{ cm}$. The received time series of magnetic field fluctuations were observed to be phase locked from shot to shot so a 5-shot ensemble average was digitized to reduce background noise.

The measured magnetic disturbances are rich in phenomena. A representative signal is shown in Fig. 3a. Initially, there is a burst of electromagnetic energy which extends beyond the upper frequency limit ($f_{\text{cutoff}} = 1.5 \text{ MHz}$) that the magnetic probes and their associated electronics can detect. Next, Alfvén waves arrive. At later times, the higher frequency Alfvén modes decay and the magnetic signal is dominated by lower frequencies.

The signal at later times ($t > 25 \mu\text{s}$) is observed to be due to standing waves which have formed along the background He plasma column. The Fourier spectrum shown in Fig. 3b displays a pronounced cutoff at the He ion cyclotron frequency as well as distinct peaks below. These peaks are similar to those observed in previous experiments on shear Alfvén resonances that were launched using an antenna driven by a current pulse [19]. The cutoff at the cyclotron frequency is what one would expect for shear Alfvén waves. The magnitude of the axial magnetic component of the wave is of the order of $1/10$ th that of the parallel and is shown as a dotted line

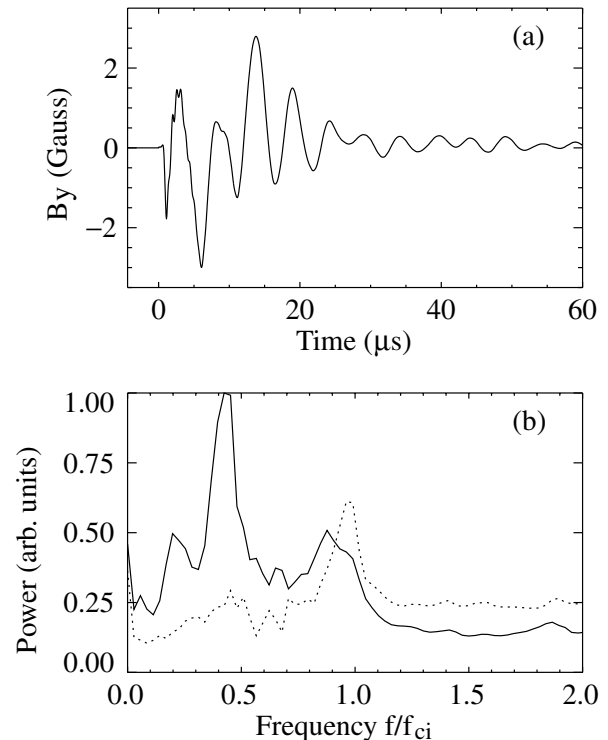


FIG. 3. (a) B_y signal obtained at $z = -31 \text{ cm}$, $x = 1.5 \text{ cm}$, $y = 2.25 \text{ cm}$. (b) The plane averaged Fourier amplitude spectrum of B_y (solid) and $10 \times B_z$ (dashed). $F_{ci} = 456 \text{ kHz}$.

in Fig. 3b. This is also characteristic of shear waves. Figure 4 shows one vector component of the wave magnetic field taken at the same x - y location in two planes separated axially by 93 cm. Initially, there is a phase delay between the signals consistent with the wave propagation time. The calculated phase velocity, using the first two minima, is $v_{\text{phase}} = 8.4 \times 10^7$ cm/s, as compared to an Alfvén speed of 9.2×10^7 cm/s in the background helium plasma ($n_0 = 2 \times 10^{12}$ cm $^{-3}$, $B_0 = 1.2$ kG). Since the wavelength ~ 400 cm is comparable to the machine length, the wave becomes a standing wave after several cycles (transit times).

A vector plot of the azimuthal wave magnetic field at $z = -124$ cm, filtered at 200 kHz ($f/f_{\text{ci}} = 0.44$), is displayed in Figs. 5a and 5b for $t = 12.1$ μs and 35.2 μs , respectively. This is a shear Alfvén wave ($B_{\perp}/B_{\parallel} \sim 10$). Initially the pattern has two distinct “O” points associated with antiparallel currents. This pattern is reminiscent of large amplitude shear waves generated in previous experiments using a helical antenna [20]. The azimuthal asymmetry of the pattern may be due to the presence of the target—a topic under investigation. Figure 5b shows the wave magnetic field after the standing mode has been set up. This mode exhibits a higher degree of azimuthal symmetry.

Since the energy of a shear Alfvén wave is contained primarily in the wave magnetic field, based on the measured fluctuating signals, an estimate can be obtained for the temporal dependence of the wave energy. As an upper limit, we integrated the total magnetic energy, over a plane located 31 cm from the target and assumed the same energy density/length for the entire length of the machine. The corresponding energy coupled into Alfvén waves is $E_A \sim 0.5\% E_{\text{Ipp}}$. The Alfvén wave radiation mechanism is complex but it could be related to the neutralizing current

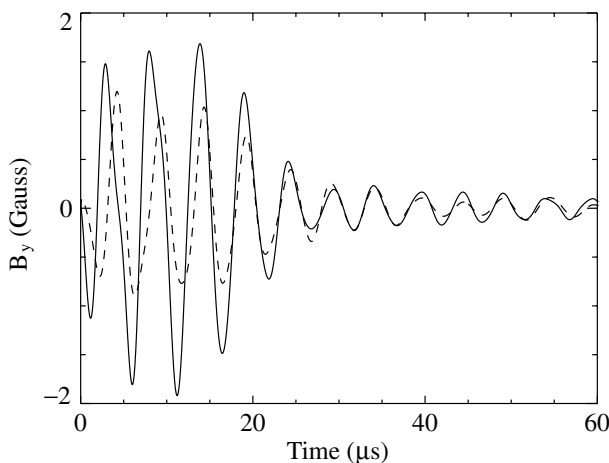


FIG. 4. The block filtered (137 kHz–456 kHz) B_y signal at two different axial locations ($z = -31$ cm and -124 cm, $x = 1.5$ cm, $y = 2.25$ cm). The phase shift is indicative of a traveling wave. The shift between the first two minima shown is 1.1 μs , giving 8.4×10^7 cm/s for the speed.

in the He background plasma that flows down the magnetic field, as discussed previously. This hypothesis is supported by the fact that E_A/E_{Ipp} is of order $(R_b \omega_{\text{pi}}/c)^2$, where $\omega_{\text{pi}} \sim 10^9$ rad/s is the ion plasma frequency of the background plasma. This hypothesis will be tested in the future with experiments and numerical simulations [17].

In summary, we have for the first time observed that Alfvén waves can be generated by a dense plasma moving through a background plasma capable of supporting them. The experiment was performed in a situation with a highly reproducible background plasma and laser-target interaction. This allowed for spatial mapping of the

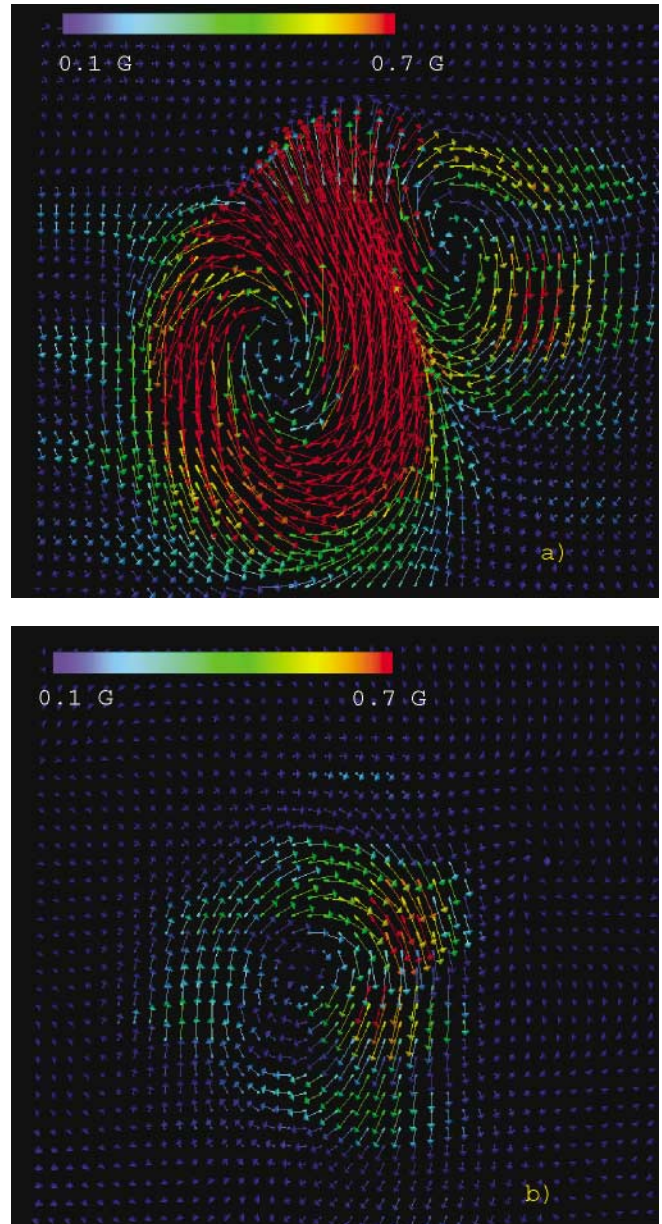


FIG. 5 (color). (a) B_{\perp} filtered at $0.44f_{\text{ci}}$, $z = -124$ cm, $t = 12.1$ μs . (b) B_{\perp} filtered at $0.44f_{\text{ci}}$, $z = -124$ cm, $t = 35.2$ μs . The arrows are 0.75 cm apart in both the horizontal and vertical directions.

wave fields and density perturbations. The laser target interaction, which ultimately gives rise to these waves, has a duration which is much smaller ($\Delta\tau_{\text{laser}}/T_{\text{wave}} \sim 10^{-3}$) than the Alfvén time scales observed. Other higher frequency waves are generated and are most likely whistler and Langmuir waves. Also, the hyperacoustic lpp ($v_{\text{lpp}}/v_{\text{ion-acoustic}} \sim 100$) should leave ion acoustic waves in its wake. Some evidence of these has been seen and will be investigated in future work. Work done in an argon background plasma has shown wave phenomena above the cyclotron frequency that displayed characteristics of compressional Alfvén waves. We will report on these in a future publication. The Alfvén waves created in our helium plasma have been identified as shear waves. After reaching the boundaries of the device, they are reflected and become standing waves. From the measured magnetic fields we estimate that 0.25% of the initial laser energy goes into these waves. Theoretically, there is also an equal amount of energy contained in the particle kinetic energy due to the wave.

The authors wish to thank G. Morales, C. Mitchell, and J. Maggs for many useful discussions. We also acknowledge the expert advice of G. Dipeso and D. Hewett and thank Livermore Labs for the use of a gated imager. This work was funded by the Department of Energy [DE-F603-98ER54494] and the Office of Naval Research [N00014-97-1-0167]. Michael VanZeeland's research was supported by Oak Ridge Institute for Science and Education under a contract between the U.S. Department of Energy and the Oak Ridge Associated Universities. The work of Guy Dimonte was performed under the auspices of the U.S. Department of Energy by the University of California, Lawrence Livermore National Laboratory under Contract No. W-7405-Eng-48.

- [1] J. T. Gosling, *Phys. Fluids B* **5**, 2638 (1993).
- [2] I. G. Richardson, E. W. Cliver, and H. V. Cane, *J. Geophys. Res.* **105**, 18 203 (2000).
- [3] H. R. Strauss, *Phys. Plasmas* **7**, 250 (2000).
- [4] R. Maingi *et al.*, *Phys. Plasmas* **4**, 1752 (1997).
- [5] G. Abel, B. Stansfield, D. Michaud, G. G. Ross, J. L. Lachambre, and J. L. Gauvreau, *Rev. Sci. Instrum.* **68**, 994 (1997).
- [6] W. Horton and W. Rowan, *Phys. Plasmas* **1**, 901 (1994).
- [7] A. Compant La Fontaine *et al.*, *Plasma Phys. Controlled Fusion* **27**, 229 (1985).
- [8] W. K. Berthold, A. K. Harris, and H. J. Hope, *J. Geophys. Res.* **65**, 2233 (1960).
- [9] Series of articles on STARFISH, *J. Geophys. Res.* **68**, 605 (1963).
- [10] H. A. Bomke, I. A. Balton, H. H. Grote, and A. K. Harris, *J. Geophys. Res.* **69**, 3125 (1964).
- [11] W. Gekelman *et al.*, *Rev. Sci. Instrum.* **62**, 2875 (1991).
- [12] D. Leneman, W. Gekelman, and J. Maggs, *Phys. Rev. Lett.* **82**, 2673 (1999).
- [13] W. Gekelman, S. Vincena, D. Leneman, and J. Maggs, *Plasma Phys. Controlled Fusion* **39**, A101 (1997).
- [14] W. Gekelman, S. Vincena, D. Leneman, and J. Maggs, *J. Geophys. Res.* **102**, 7225 (1997).
- [15] Guy Dimonte and L. G. Wiley, *Phys. Rev. Lett.* **67**, 1755 (1991).
- [16] B. Meyer and G. Thiell, *Phys. Fluids* **27**, 302 (1984).
- [17] G. Dipeso and D. Hewett (private communication).
- [18] T. H. Tan, G. H. McCall, and A. H. Williams, *Phys. Fluids* **27**, 296 (1983).
- [19] C. Mitchell, S. Vincena, J. E. Maggs, and W. N. Gekelman, *Geophys. Res. Lett.* **28**, 923 (2001).
- [20] W. Gekelman, S. Vincena, D. Leneman, and J. Maggs, *Plasma Phys. Controlled Fusion* **42**, B15 (2000).